Journal of Innovative Optical Health Sciences
Vol. 8, No. 5 (2015) 1550024 (9 pages)

DOI: 10.1142/S1793545815500248

World Scientific
www.worldscientific.com

Effect of head model on Monte Carlo modeling of spatial sensitivity distribution for functional near-infrared spectroscopy

Ting Li*,‡, Yan Li†, Yunlong Sun*, Meixue Duan* and Liyuan Peng*
*State Key Lab Elect Thin Film & Integrated Device and Department of Biomedical Engineering, University of Electronic Science & Technology of China, Chengdu 610054, P. R. China
†Design Department No. 2, Avic Beijing Keeven Aviation Instrument Co. Ltd, Beijing 100086, P. R. China
‡liting@uestc.edu.cn

Received 28 September 2014
Accepted 1 December 2014
Published 31 December 2014

Modeling Light propagation within human head to deduce spatial sensitivity distribution (SSD) is important for Near-infrared spectroscopy (NIRS)/imaging (NIRI) and diffuse correlation tomography. Lots of head models have been used on this issue, including layered head model, artificial simplified head model, MRI slices described head model, and visible human head model. Hereinto, visible Chinese human (VCH) head model is considered to be a most faithful presentation of anatomical structure, and has been highlighted to be employed in modeling light propagation. However, it is not practical for all researchers to use VCH head models and actually increasing number of people are using magnet resonance imaging (MRI) head models. Here, all the above head models were simulated and compared, and we focused on the effect of using different head models on predictions of SSD. Our results were in line with the previous reports on the effect of cerebral cortex folding geometry. Moreover, the influence on SSD increases with the fidelity of head models. And surprisingly, the SSD percentages in scalp and gray matter (region of interest) in MRI head model were found to be 80% and 125% higher than in VCH head model. MRI head models induced nonignorable discrepancy in SSD estimation when compared with VCH head model. This study, as we believe, is the first to focus on comparison among full serials of head model on estimating SSD, and provided quantitative evidence for MRI head model users to calibrate their SSD estimation.

Keywords: Visible chinese human; functional near-infrared spectroscopy; Monte Carlo simulation; head model; spatial sensitivity distribution.

‡Corresponding author.

1. Introduction

Characterization of human tissue blood oxygenation, blood volume, and blood flow in brain is important for diagnosis and therapeutic assessment of brain function and vascular/cellular diseases.[1–4] Near-infrared spectroscopy (NIRS) and imaging (NIRI) have been applied to measure changes of blood oxygenation and volume of the brain tissue, which are caused by functional brain activity.[1,2,5] These traditional NIRS has been already widely accepted by research and clinics as a simple, fast, portable, low-cost, and nonionizing technique for noninvasive quantification of blood oxygenation-represented brain functional activities. An emerging dynamic NIR methodology, diffuse correlation spectroscopy (DCS),[3,4] has been developed to measure blood flow in brain microvasculature. Recently, DCS has been combined with NIRS in hybrid instruments and truly portable models.[4] Challenge remains for all these techniques in the precision or spatial resolution. Precise modeling of light propagation in the head to deduce the spatial sensitivity profile is crucial to improve precision/spatial resolution of all the above NIR technologies.[3,4,6,7]

The heterogeneity of the tissues in human head, especially the space filled with cerebrospinal fluid (CSF) has been found to strongly affect light propagation in the brain.[8–10] Moreover, since the brain surface is folded and filled with CSF, It is straightforward to question if and how the complex geometry of the brain surface affects the light propagation in human head. Some researchers have published studies on this issue, by using artificial head models[7,8] generated from MRI scan,[8–15] and visible chinese human (VCH) head model.[10] Some studies concluded that the cerebral cortex folding geometry has little effect, if any, on light propagation,[8–12] while Ref. 16 reported substantial effect of cerebral cortex folding geometry on light propagation. The volume of tissue contributing to the change in the intensity of the detected light was obtained as the spatial sensitivity profile/distribution (SSD), which is calculated from the accumulated trajectories of the detected light.[7] Accordingly, it is reasonable for us to question if the fidelity of those head models biased the estimation of light propagation, especially e.g., SSD.

In particular, with the spread of MRI in both clinical and research usages, it became easier for us to get MRI datasets for head modeling. On the other side, the VCH head model is the most faithful representation of human head structure,[17] however, it is not easy or straightforward to obtain the VCH dataset, as well as to construct the head model with the dataset. As a consequence, more and more studies employed the MRI slices to obtain the head model in their light propagation simulation and computation of SSD. With these facts, the deviation of MRI-based head model from the faithful head model (e.g., VCH head model) in light propagation simulation, which makes us more cautious of calculations of SSD based on MRI-based head model for our NIRS and DCS uses, is taken into account. A quantification of the deviation in estimates of SSD based on head models between MRI slices and VCH datasets is essential.

In this study, light propagations in a series of head models were predicted and compared. The head models included a layered head model, an artificial layered head model with slots mimicking sulci, a three-dimensional (3D) MRI-based head model, and the VCH head model[18,20] whose fidelity is significantly higher than MRI-based models.[17–20] The first three models were originated from the previous reports. The spatial sensitivity profiles in the previous three head models were initially compared with previous studies to validate simulation results. Then, the spatial sensitivity profiles or distributions in the 3D MRI-based head model and the VCH head model were compared with the above data, exploring if the fidelity of head model has a strong effect on predicting the SSD. Especially, the distinction in SSD computed based on differences between 3D MRI-based head model and VCH head model were addressed/quantified, by comparison on 3D color maps and pie plot for percentages of SSD within different types of tissue. Finally, the effects of the fidelity of head model were discussed.

2. Method

2.1. *Head models*

Figure 1 showed the head models used in this study, including a widely used layered head model (1D), two different-scale artificial head models containing slots simulating the brain surface and gray-white matter interface (2D), Zubal head model (3D), and VCH head model (3D). Thereinto, Zubal model is a widely used voxel-based anthropomorphic phantom generated from MRI scans.[21,22] The spatial

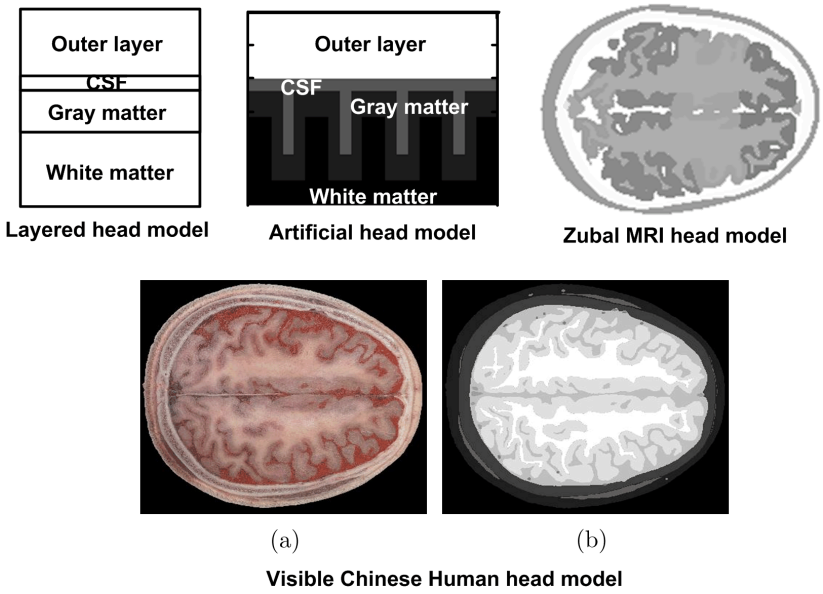

Fig. 1. Head models. VCH head model: (a) Digital color photograph of one head slice in the VCH dataset; (b) Segmentation of the slice in (a).

resolution of Zubal MRI model equaled $0.11 \times 0.11 \times 0.14\,\text{cm}^3$.[21–23]

The VCH dataset was newly developed according to high-resolution cryosectional color photographs of a reference adult male.[16–19] Briefly, the VCH specimen, a male adult, was frozen in the standing posture, and horizontally sectioned at 0.02-cm interval. Digital color photographs of the top surface after each sectioning were obtained with the resolution of 0.01-cm per pixel (shown Fig. 1(a) as an example), which is higher than CT or MRI data (such as Zubal model[21–23]). Following a fine segmentation supervised by anatomists, a voxelized model (voxel size: $0.01 \times 0.01 \times 0.02\,\text{cm}^3$) that most faithfully represented the human anatomical structures was established[10–12,16] (shown Fig. 1(b) as an example). The segmentation of VCH, unlike CT or MRI data, was performed based on these color photographs, with little dependence on pixel gray values. The advantages, including high resolution and precise segmentation, make the VCH the most faithful representation of human anatomical structures. Particularly, the upstanding posture of VCH, instead of lying down in MRI or CT, was able to present verisimilar geometry of brain surface geometry/CSF layers for light propagation prediction. Comparatively, the approximate thickness of the CSF layer in the region of interest were distinct as shown in Fig. 1, although highly-varied, roughly ~3 mm for Zubal and ~5 mm for VCH head model.

The optical properties for each tissue in head models above were listed in Table 1.[7–10,24–26] The optical properties for those tissues, including scalp, skull, CSF, gray matter, and white matter, were the same as those used by most references.

2.2. *Monte Carlo simulations*

Monte Carlo simulation was utilized to calculate light propagation in the head models. Here, we used the Monte Carlo simulation software targeted for voxelized media (MCVM), the algorithm of which has been described in Ref. 27. To simulate NIRS/NIRI, the light source ("S") and detector ("D") were located on the surface of the forehead of head models at 1 cm above the eyebrows with a 3.7-cm

Table 1. Optical properties of head tissues for 800-nm light.

Tissue type	μ_a (cm^{-1})	μ_s (cm^{-1})	g	n
Scalp	0.18	190	0.9	1.37
Skull	0.16	160	0.9	1.43
Muscle	1.40	500	0.9	1.4
CSF[a]	0.04	24	0.9	1.33
Arterial blood	2.33	500	0.99	1.4
Venous blood	2.38	522	0.99	1.4
Gray matter	0.36	220	0.9	1.37
White matter	0.14	910	0.9	1.37

Note: [a]Cerebrospinal fluid.

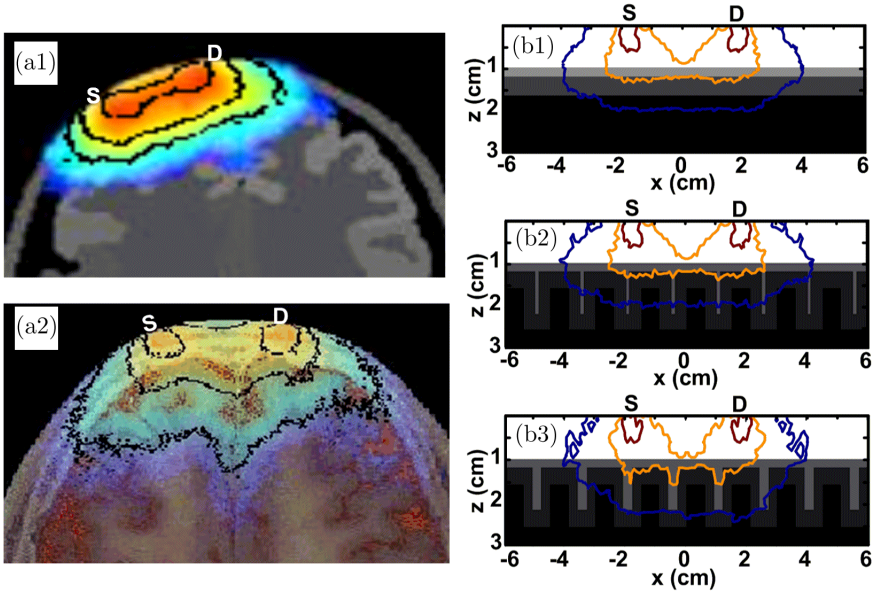

Fig. 2. Spatial sensitivity profiles in the Zubal MRI head model (a1) and VCH head model (a2), layered head model (b1) and artificial head models (b2), (b3) derived from the paper of Okada.[10] The separation between light source and detector in each model equaled 3.7 cm. The width of slots in (b3) is triple of that in (b2).

separation (see Figs. 2 and 3). Based on our previous study for SSD simulations at different separations in the range of (1.5, 51) cm,[16] we found that for large separations (e.g., 5.1 cm) and for small separations (e.g., <2.4 cm) SSD simulations were not as strong as those in the range of (3.3, 4.2) cm affected by geometry details of cerebral cortex. We got to know that the separation in the range of (3.3, 4.2) cm showed the strongest effect of cerebral cortex geometry on SSD and thus we choose the intermediate separation of 3.7 cm in this simulation study. For the realistic models, the light sources and detectors were placed on the frontal head, located in the slice (Fig. 1) about 1 cm above the eyebrows. Ten million photons were injected on each head model. Each simulation was performed 10 times and finally the simulation results were averaged for data analysis. The spatial sensitivity profiles in each head model were accumulated for comparisons. Here SSD is defined and calculated as the transport from the source to an x, y, z position times the transport from the same x, y, z position to the detector. MCVM enabled simulation of light propagation in both time-resolved and stable-state. Here, we only performed the stable-state simulation since there are more continuous-wave modalities of NIRS than time- or frequency- domain NIRS.

3. Results

Simplified head models employed by Okada *et al.*[7,8] were firstly tested by our Monte Carlo simulation [Fig. 2(b1) and 2(b2)]. The gray lines in Fig. 2(b1) denoted the interface between different tissues in the layered head model including the outer layer, CSF, white matter, and gray matter. Figure 2 displays the SSD in a transverse section at z equal to 1 cm above the eyebrows, for the placements of the source and detector. In the figures, the contours are drawn for 10%, 1% and 0.1% of the maximum S of each image. The maximum S values for Figs. 1(b) and 1(c) are $8.4 \times 10^{-4}\,\mathrm{cm}^{-4}$ and $9.7 \times 10^{-4}\,\mathrm{cm}^{-4}$, respectively.

Figures 2(b1) and 2(b2) show the results of the Monte Carlo simulation using the simplified head models of Okada.[8,10] The same contours for 10%, 1%, and 0.1% of maximum S are drawn for Fig. 2 (b1) no sulci, and for (b2) a thin 1-mm sulci, which repeated the calculations of Okada. To consider larger sulci, a third simulation in Fig. 2(b3) used a thick 3-mm sulci. The maximum S values for Figs. 2 (b1)–2(b3) are $2.9 \times 10^{-4}\,\mathrm{cm}^{-4}$, $2.1 \times 10^{-4}\,\mathrm{cm}^{-4}$, and $1.7\times 10^{-4}\,\mathrm{cm}^{-4}$, respectively.

Note that the 1% contour in Fig. 2(a2) manages to penetrate the 3-mm sulci, but fails to penetrate the 1-mm sulci of Fig. 2(b3). The depth of the 0.1% contour is ~3.3-mm greater for the 3-mm sulci (~2.23 cm) than for the 1-mm sulci (~1.90 cm) or

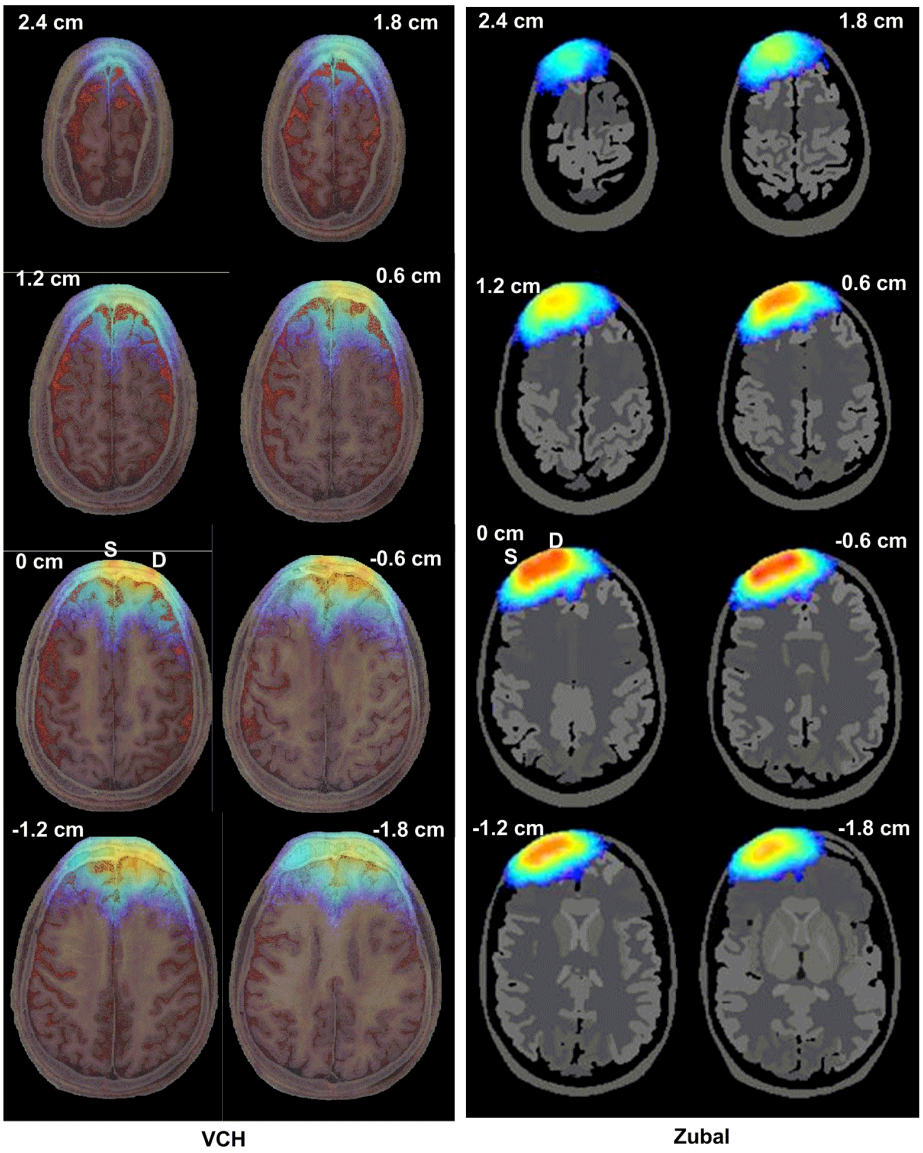

Fig. 3. SSD in VCH and Zubal head models, respectively. The separation of light source and detector is 3.7 cm.

no sulci (∼1.90 cm). The sulci in the Zubal MRI head model [Fig. 2(a1)] are similar or a little bit larger than the 0.3-cm sulci of the simplified model. The penetration of the 0.1% contour into the central sulcus was not that significant. As for VCH head model, most sulci are larger than the 0.3-cm sulci of the simplified model, especially the central sulcus at the midline. The penetration of the 1% and 0.1% contour into the sulci (especially the central sulci) are dramatic [Fig. 2(a2)]. The depth of the 0.1% contour is around ∼3.5 cm in Zubal head model, while around 4 cm in VCH head model. The distortion of the SSD around the brain surface on the VCH head model is much stronger than both simplified head models and Zubal MRI head model.

For further comparison between Zubal MRI head model and VCH head model influencing the SSD estimates, we first visualized the 3D SSD for both head models. Figure 3 shows the transverse sections of SSD through the head at differential height marked on the subfigures for comparison between MRI-based and VCH-based head model. The spatial sensitivity profiles on Zubal head model (Fig. 3) did repeat the previous findings on MRI-based head models[8,9,11,12] as well. The SSD were a little distorted for MRI-based head model by the brain structure, while for VCH head model, the SSD

distorted substantially by the brain structure. The penetration depth fluctuated significantly along the brain surface, and was shown to be larger in the region through deeper brain surface under the source–detector pair.

Based on the 3D SSD data from both head models, we accumulated the SSD in each voxel by each type of tissue and showed the percentage values by pie plots. Figure 4 shows the pie plots of SSD within each type of tissue in total for the two head models, respectively in terms of percentages. The percentages of SSD in scalp and gray matters are significantly overestimated in Zubal MRI head model compared to those in VCH head model (by $>80\%$ in scalp; by 125% in gray matter). While the percentage of SSD in CSF layer is extremely underestimated in Zubal MRI head model compared to that in VCH head model (by 96%). The results mean, surprisingly, that researchers may have to take care of the deviation if they used MRI head model in their SSD calculation. And the above quantification of the deviation can be used as reference to calibrate the SSD calculation based on MRI head model. For example, since that the Zubal MRI head model based calculation of SSD in gray matter doubled that in VCH head as shown in Fig. 4, we may cut the results based on Zubal MRI head model in half.

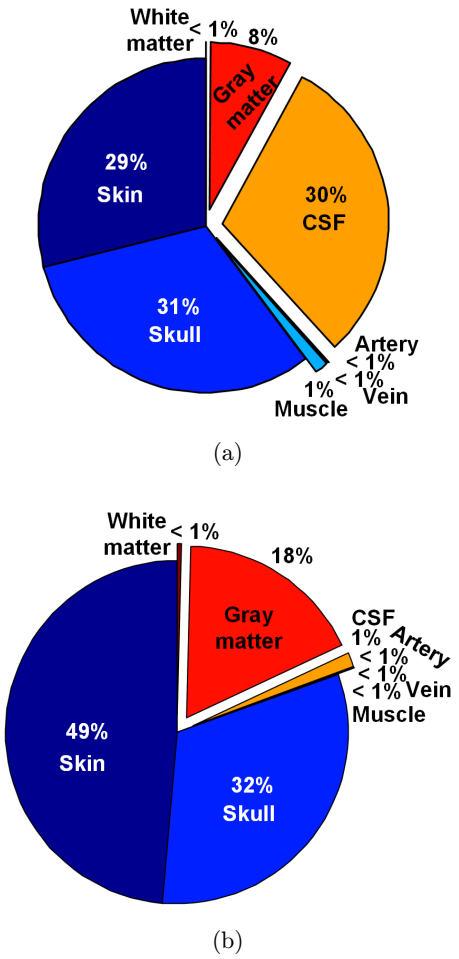

Fig. 4. Pie of SSD in each tissue layers in VCH (a) and Zubal MRI (b) head models, respectively.

By comparison on the distortion of SSD in the geometry of the brain among all head models, we could observe that the distortion strengthened with the enhancement of fidelity of the head models. Accordingly, the effect of cerebral cortex folding geometry on light propagation was underestimated by previous researches on those head models with lower fidelity. The Zubal head model, which was a 3D MRI-based head model with much higher fidelity than the artificial head models or 2D head model based on a single MRI scan, was still not realistic enough for studying the effect of cerebral cortex folding geometry on light propagation.

4. Conclusion and Discussion

The light propagation in a layered head model, an artificial head model with sulci slots, Zubal MRI head model, and VCH head model was computed by Monte Carlo method, the fidelity of which increased successively. Among these models, MRI-based 3D head model has been in use more and more often, while the VCH is known as the most realistic head model. The SSD in layered, artificial simplified 2D head model, and Zubal MRI head model agreed with the previous reports[5–9] that the complex geometry of the brain surface has no or small effect on light propagation into the human head. However, we observed that the distortion of the brain structure enhanced with the fidelity of the head model while the spatial sensitivity profile in VCH head model showed strong effects on the complex brain structure. This finding indicated that the fidelity of head model produces significant influence on SSD estimation for NIRS and DCS.

Further, this study is the first to attempt to provide a quantitative comparison between SSD estimates from MRI-based head model and VCH head model. MRI-based head model is not precise as VCH head model. However, MRI-based head model has achieved increasing use nowadays, which might

be due to the spreading of MRI equipments in both hospitals and research labs all over the world and thus the easier acquisition of MRI datasets. While VCH dataset is neither easy to obtain nor straightforward to follow and establish the head model using the huge VCH datasets. The deviation between SSD estimates from the two head models was not quantitatively clear. Our study targeted this issue and provided quantitative comparison on SSD estimates from the standard Zubal MRI head model and VCH head model. Our results show that the percentages of SSD are highly overestimated in Zubal MRI head model compared to those in VCH head model in scalp and NIRS/DCS-interested gray matters (by $>80\%$ in scalp; by 125% in gray matter), while the percentage of SSD in the CSF layer is extremely underestimated in Zubal MRI head model (by 96%). We therefore remind that researchers may have to take care of the deviation if they employed MRI head model in SSD estimation. Moreover, our quantification of the deviation in SSD estimates between Zubal MRI head model and the most-faithful human structure represented VCH head model provides a reference for the SSD calibration based on MRI head model.

In the VCH head model, the SSD distorted obviously around the curved brain surface, and the penetration depth fluctuated significantly along the brain surface. As you can clearly observe from our data and our previous publication,[16] the effect of cerebral cortex geometry on light propagation is enhanced by the effect of CSF layer which was filled in the crooked and various shades of cerebral cortex sulcus. Moreover, the effect of cerebral cortex geometry on light propagation was seen as increasing with the fidelity of the head model. Hence, the effect of complex brain structure on light propagation in human head is greater than it was previously recognized. Accordingly, high-fidelity head models, such as VCH head model, are recommended to be utilized in the studies on light propagation in human head, especially on the issues concerning the complex brain geometry. Illustrated by the simulation results with VCH head model, the sensitivity of local brain activity to NIRS signal may be determined by not only the depth of the activated region from the source–detector pair but also the depth of the brain surface upon the local point.

The size of sulci proved to be an important factor in complex geometry of the brain surface in affecting the light propagation in human head. When the sulci size was small (1 mm), the cerebral cortex folding geometry did not show obvious effect on the light propagation [Fig. 2(b2)]; however, when the sulci size increased to 3 mm, the cerebral cortex folding geometry did show significant effect on the light propagation [Fig. 2(b3)]. Especially, on the VCH head, when the sulci size increased to be larger than 3 mm in some region (like the central sulci), the effect of the cerebral cortex folding geometry strengthened [Figs. 2(a1) and 2(a2)]. Therefore, the underestimation of sulci size caused underestimation of the effect of head model on the light propagation.

The variation in the size, geometry, and 3D distribution of the sulcus in the whole human head also had an effect on the light propagation. For Zubal model, mainly because of its lower resolution than the VCH head model, the size and geometry of its sulcis were likely to be not as realistic as the VCH head model. Moreover, because of the low resolution in the Zubal head model, those sulcis with smaller size than single voxel were possibly eliminated and those sulcis at size of 1–2 voxels were reduced to one voxel. Accordingly, the size of many sulcus was underestimated in MRI head model. That would be the reason for less effect by brain geometry on light propagation in Zubal head model, compared with the VCH head model. Of note, since the 3D distribution of the sulci differed among individuals, and since the Zubal model was in lying posture while the VCH model was in standing posture in sample preparation, which introduced difference in cerebral geometry between them, it is reasonable that the SSD differed between the Zubal and VCH head models.

This study represented a good advance that will somewhat affect future studies on SSD estimation by other investigators, but these theory results performed by MC simulations shown in this work should be supported and verified by careful experimental measurements and/or with other methods of simulation, e.g., numerical diffusion forward model. In addition to this Monte Carlo simulation study, the diffusion forward model based on the finite element and volume methods is worthy of further study to provide more reliable and quantitative evidence to researchers for their better choice of head model. Further quantitative analysis on the light transport in realistic head models taking advantage of the low scattering and absorption coefficients observed in CSF is also requisite. In addition, considering that there were different diffuse optical DOT systems, further studies expanding our scope

of work all the time, CW and frequency techniques could be intriguing.

In summary, this study computed SSD with Monte Carlo simulation using a series of head models employed in NIRS/DCS field. The comparison among the results indicated that the fidelity of head models affected the SSD estimation significantly. VCH head model is quite recommended in use. Since MRI-based head model is increasingly used due to increased availability of MRI equipment and it is easy to get and follow MRI data in modeling head structure, we compared MRI-based head model with VCH head model in SSD estimates quantitatively, but it is a pity that there is no subject with both VCH data and MRI data. We therefore could not use an identical subject in this study. However, considering that both Zubal MRI model and VCH model are identified in tissue segmentation, using Zubal head model and VCH head model is the best way we can do at the current stage. Surprisingly we found that MRI-based head model could induce 125% overestimation in NIRS/DCS targeted gray matter and 96% underestimation in CSF layer. This quantitative deviation by Zubal MRI-based head model reminds us to take care whilst using MRI head model in calculating SSD and guide us better to calibrate MRI head model produced SSD.

Acknowledgment

The authors thank Qingming Luo's group for providing VCH dataset. This research was supported by the Fundamental Research Funds for the Central Universities (grant No. ZYGX2012J114), the National Natural Science Foundation of China (grant No. 61308114) and the Specialized Research Fund for the Doctoral Program of Higher Education (grant No. 20130185120024).

References

1. A. Villringer, B. Chance, "Non-invasive optical spectroscopy and imaging of human brain function," *Trends Neurosci.* **20**, 435–442 (1997).
2. Y. Hoshi, "Functional near-infrared spectroscopy: Current status and future prospects," *J. Biomed. Opt.* **12**, 062106 (2007).
3. G. Yu, T. Durdurn, C. Zhou *et al.*, "Noninvasive monitoring of murine tumor blood flow during and after photodynamic therapy provides early assessment of therapeutic efficacy," *Clin. Cancer Res.* **11**, 3543–3552 (2005).
4. T. Li, Y. Lin, Y. Shang *et al.*, "Simultaneous measurement of deep tissue blood flow and oxygenation using noncontact diffuse correlation spectroscopy flow-oximeter," *Sci. Rep.* **3**, 1358 (2013).
5. T. Li, Q. Luo, H. Gong, "Gender-specific hemodynamics in prefrontal cortex during a verbal working memory task by near-infrared spectroscopy," *Behav. Brain Res.* **209**, 148–153 (2010).
6. Y. Shang, T. Li, L. Chen, Y. Lin, M. Toborek, G. Yu, "Extraction of diffuse correation spectroscopy flow index by integration of Nth-order linear model with Monte Carlo simulatiion," *Appl. Phys. Lett.* **104**, 193703 (2014).
7. Y. Fukui, Y. Ajichi, E. Okada, "Monte Carlo prediction of near-infrared light propagation in realistic adult and neonatal head models," *Appl. Opt.* **42**, 2881–2887 (2003).
8. E. Okada, D. T. Delpy, "Near-infrared light propagation in an adult head model. I. Modeling of low-level scattering in the cerebrospinal fluid layer," *Appl. Opt.* **42**, 2906–2914 (2003).
9. Y. Ogoshi, E. Okada, "Analysis of light propagation in a realistic head model by a hybrid method for optical brain function measurement," *Opt. Rev.* **12**, 264–269 (2005).
10. E. Okada, M. Firbank, M. Schweiger, S. R. Arridge, M. Cope, D. T. Delpy, "Theoretical and experimental investigation of near-infrared light propagation in a model of the adult head," *Appl. Opt.* **36**, 21–31 (1997).
11. G. Strangman, M. A. Franceschini, D. A. Boas, "Factors affecting the accuracy of near-infrared spectroscopy concentration calculations for focal changes in oxygenation parameters," *NeuroImage* **18**, 865–879 (2003).
12. D. A. Boas, A. M. Dale, "Simulation study of magnetic resonance imaging-guided cortically constrained diffuse optical tomography of human brain function," *Appl. Opt.* **44**, 1957–1968 (2005).
13. M. Chemseddine, L. H. Jean-Pierre, H. K. Nasser, H. Anne, "Depth sensitivity analysis of functional near-infrared spectroscopy measurement using three-dimensional Monte Carlo modelling-based magnetic resonance imaging," *Lasers Med Sci.* **25**, 431–438 (2010).
14. C. Chuang, C. Chen, Y. Hsieh, T. Liu, C. Sun, "Brain structure and spatial sensitivity profile assessing by near-infrared spectroscopy modeling based on 3D MRI data," *J. Biophotonics* **6**, 267–274 (2013).
15. C. Mansouri, N. H. Kashou, "Spatial sensitivity of near-infrared spectroscopic brain imaging based on

three-dimensional monte carlo modeling," *Conf. Proc. IEEE. Eng. Med. Biol. Soc.* **2009**, 1457–1460 (2009).
16. T. Li, H. Gong, Q. Luo, "Visualization of light propagation in visible Chinese human head for functional near-infrared spectroscopy," *J. Biomed. Opt.* **16**, 045001 (2011).
17. G. Zhang, Q. Luo, S. Zeng, Q. Liu, "The development and application of the visible Chinese human model for Monte Carlo dose calculations," *Health Phys.* **94**, 118–125 (2008).
18. D. Han and Q. Liu, Available at: http://202.114.29.53/VCH/Humen/index.aspx (2005).
19. S. X. Zhang, P. A. Heng, Z. J. Liu, L. W. Tan, M. G. Qiu, Q. Y. Li, R. X. Liao, K. Li, G. Y. Cui, Y. L. Guo, X. P. Yang, G. J. Liu, J. L. Shan, J. J. Liu, W. G. Zhang, X. H. Chen, J. H. Chen, J. Wang, W. Chen, M. Lu, J. You, X. L. Pang, H. Xiao, Y. M. Xie, J. C. Cheng, "The Chinese Visible Human (CVH) datasets incorporate technical and imaging advances on earlier digital humans," *J. Anat.* **204**, 165–173 (2004).
20. A. Li, Q. Liu, S. Zeng, L. Tang, S. Zhong, Q. Luo, "Construction and Visualization of high-resolution three-dimensional anatomical structure datasets for Chinese digital human," *Chin. Sci. Bull.* **53**, 1848–1854 (2008).
21. I. G. Zubal, C. R. Harrell, E. O. Smith, Z. Rattner, G. Gindi, P. B. Hoffer, "Computerized three-dimensional segmented human anatomy," *Med. Phys.* **21**, 299–302 (1994).
22. V. Toronov, E. D'Amico, D. Hueber, E. Gratton, B. Barbieri, A. Webb, "Optimization of the signal-to-noise ratio of frequency-domain instrumentation for near-infrared spectro-imaging of the human brain," *Opt. Express* **11**, 2717–2729 (2003).
23. Yale Medicine School, Available at http://noodle.med.yale.edu/phantom/getmridesc.htm
24. W. F. Cheong, S. A. Prahl, A. J. Welch, "A review of the optical properties of biological tissues," *IEEE J. Quantum. Electron.* **26**, 2166–2185 (1990).
25. A. N. Yaroslavsky, P. C. Schulze, I. V. Yaroslavsky, "Optical properties of selected native and coagulated human brain tissues in vitro in the visible and near infrared spectral range," *Phys. Med. Biol.* **47**, 2059–2073 (2002).
26. E. Okada, D. T. Delpy, "Near-infrared light propagation in an adult head model. II. Effect of superficial tissue thickness on the sensitivity of the near-infrared spectroscopy signal," *Appl. Opt.* **42**, 2915–2922 (2003).
27. T. Li, Q. Luo, H. Gong, "MCVM: Monte Carlo modeling of photon migration in voxelized media," *J. Innov. Opt. Health. Sci.* **3**, 91–102 (2010).